PHYSICAL REVIEW B VOLUME 41, NUMBER 7 1 MARCH 1990

Soft-x-ray emission spectroscopy study of La_2CuO_4 and three high-T_c superconductors

V. Barnole, J.-M. Mariot, and C. F. Hague
Laboratoire de Chimie Physique, Université Pierre et Marie Curie, 11 Rue Pierre et Marie Curie, F-75231 Paris CEDEX 05, France

C. Michel and B. Raveau
*Laboratoire de Cristallographie et Sciences des Matériaux, Institut des Sciences de la Matière et du Rayonnement,
Bld. du Maréchal Juin, F-14032 Caen CEDEX, France*

(Received 30 May 1989; revised manuscript received 23 October 1989)

High-resolution x-ray emission spectroscopy measurements have been performed on sintered samples of La_2CuO_4, $La_{1.85}Sr_{0.15}CuO_{4-\delta}$, $YBa_2Cu_3O_{7-\delta}$ ($\delta < 0.1$), and compressed polycrystalline $Bi_2Sr_2CaCu_2O_{8+\delta}$. The Cu $L\alpha$ and O $K\alpha$ emission bands, which reflect the local partial Cu 3d and O 2p states, respectively, are compared to photoelectron spectra and ground-state local-density-approximation (LDA) densities-of-states (DOS) calculations. Our results show that solid-state effects are dominant. In particular, the differences in shape of the O $K\alpha$ emission bands follow the trends predicted by LDA, although it must be stressed that they mainly arise from O 2p states at oxygen sites not directly involved in the Cu-O planes. The Cu-side 3d states, on the other hand, vary little from one cuprate to the next and are more strongly localized than expected from LDA predictions. The Anderson-impurity model calculations of Kotani and co-workers are discussed, and it is concluded that they provide a satisfactory explanation of the Cu $L\alpha$ emission data, which reflect strong on-site Coulomb interaction. We conclude that the apparently good agreement between LDA-calculated DOS and low-energy photoemission experiments recently reported results from the high sensitivity of the latter to O 2p states. Discrepancies are to be expected in excitation spectra that involve mainly 3d electrons.

I. INTRODUCTION

The majority of experimental studies on the electronic structure of high-T_c superconductors has relied on x-ray photoelectron spectroscopy (XPS), ultraviolet photoelectron spectroscopy (UPS), or photoelectron spectroscopy (PES) performed at intermediate excitation energies by means of monochromatized synchrotron radiation (see, for instance, Refs. 1–10). High-resolution UPS performed below T_c has recently revealed the presence of a superconducting gap in $Bi_2Sr_2CaCu_2O_8$ single crystals[6–8] as predicted by BCS theory. Other very recent PES data[9,10] tend to support the single particle picture of the local-density approximation (LDA) to the density-functional theory. This comes at a time when efforts are being made to include on-site Coulomb interaction to help interpet just such experiments.[11–13] This is certainly a major issue since the size of the Coulomb interaction is an important ingredient of the theoretical models currently being developed to explain the magnetic and superconducting properties of these compounds (see, for instance, Ref. 14). We know that the bulk of the valence electrons belongs to the Cu-O network so the first step is to determine the degree of localization or hybridization of the Cu 3d states and O 2p states.

To a certain extent such information is forthcoming from the valence-band densities of states (DOS) obtained from PES experiments because the photoionization cross sections for Cu 3d and O 2p electrons vary differently with photon energy (see Ref. 10). A more directly site selective technique is provided, however, by x-ray emission spectroscopy (XES) since it involves transitions to a localized core hole within the potential well of a particular ionized atom (see, for instance, Ref. 15). To be more precise XES probes the local DOS averaged over all the sites of each constituent element separately and, because dipole selection rules apply, the x-ray emission process is also symmetry selective. It follows that the Cu $L\alpha$ ($3d \rightarrow 2p_{3/2}$) and O $K\alpha$ ($2p \rightarrow 1s$) x-ray emission bands can provide unique information on the local partial Cu 3d and O 2p electronic structure in these complex materials. Compared to PES experiments, very few XES experiments on high-T_c materials have been reported so far.[15–22]

In this paper we compare high-resolution x-ray emission spectra from three classes of perovskite-type superconductors. The superconductors investigated are $La_{1.85}Sr_{0.15}CuO_{4-\delta}$, $YBa_2Cu_3O_{7-\delta}$ ($\delta < 0.1$), and $Bi_2Sr_2CaCu_2O_{8+\delta}$; they are hereafter referred to as La-Sr-Cu-O, Y-Ba-Cu-O, and Bi-Sr-Ca-Cu-O, respectively. In addition we examine an undoped semiconducting La_2CuO_4(La-Cu-O) sample. In Sec. II we briefly draw attention to some difficulties which are encountered in such experiments and the results are presented in Sec. III. The discussion (Sec. IV) underlines the main discrepancies between ground-state LDA calculations and our observations. We assess the initial and final state ionization effects which partly explain these differences with the aim that XES may ultimately serve as a test for the proper inclusion of electronic correlation in LDA calculations.

II. EXPERIMENTAL

Sintered samples were prepared by now standard procedures.[23,24] Superconducting La-Sr-Cu-O was obtained by annealing at 400 °C for 24 h under O_2 at atmospheric pressure. The Bi-Sr-Ca-Cu-O sample was a compressed polycrystalline pellet. Samples were bonded with silver paste to a chromium plated water-cooled copper holder and inserted into the x-ray source chamber of a Johann spectrometer[25] via a fast insertion lock. They were lightly scraped with a diamond file just prior to measurement. The residual pressure during measurements was below 2×10^{-7} mbar.

We found that rubidium acid pthalate (RbAP), among the phthalate crystals, gave the best results for recording the O $K\alpha$ emission bands despite the proximity of two regions of rapidly varying reflectivity. One is situated at ~532 eV and the other lies at ~521 eV. The former variation in reflectivity lies sufficiently above the emission band not to affect the spectrum, but the second more seriously modifies the shape of spectra towards low x-ray transition energies. Quite fortuitously, at relatively low resolution settings, the shape of the O $K\alpha$ emission band for Y-Ba-Cu-O measured with RbAP (Ref. 17) or a grating spectrometer[18] are very similar. To illustrate these experimental artifacts we compare (Fig. 1) the O $K\alpha$ emission band for BeO measured with RbAP and measured with a grating spectrometer.[26] The O 2p bonding states show up as a low intensity shoulder at ~522 eV in the grating measurements but are deformed when studied with RbAP by a dip in reflectivity close to the main line and a reinforced intensity ~5 eV below the main line. If the main line is broad or the resolving power is reduced the low-energy part of the spectrum appears as a shoulder to the main line. We used RbAP despite this shortcoming because its reflectivity is high.[27,28] To obtain similar results with a grating spectrometer would require much higher power applied to the sample (see Ref. 26).

Thanks to improved sample cooling we were able to increase the power of the electron beam excitation from 1 (our previous measurements) to 2.4 W without any deterioration of the sample over long periods of time. Hence, improved experimental resolution could be obtained while maintaining short (1–2 h) measuring times. A beryl crystal was used to record the Cu $L\alpha$ emission. The instrumental resolution was estimated to be 0.5 and 0.3 eV, respectively, for the O $K\alpha$ and Cu $L\alpha$ emission bands. The excitation potential used was 4 and 3 kV, respectively, for the O $K\alpha$ and Cu $L\alpha$ emissions which meant that the effective thickness probed was ~1000 Å.

The energy scales were carefully calibrated using refer-

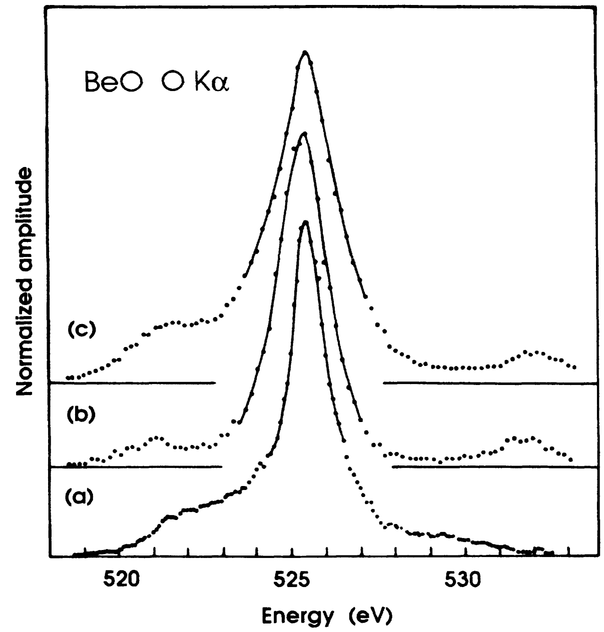

FIG. 1. O $K\alpha$ emission band for BeO with (a) grating (Ref. 26); (b) RbAP (~0.5 eV instrumental broadening); (c) RbAP (~1 eV instrumental broadening). Variations in the RbAP reflection coefficient are observed at ~521 eV and ~532 eV.

TABLE I. Cu 3d and O 2p binding energies from XPS Cu $2p_{3/2}$ and O 1s binding energies (selected values) and XES Cu $L\alpha$ and O $K\alpha$ emission band energies. The XPS and UPS valence-band (VB) peak positions are also given for comparison. (All values in eV).

	CuO	La-Cu-O	La-Sr-Cu-O	Y-Ba-Cu-O	Bi-Sr-Ca-Cu-O
Cu $2p_{3/2}$	933.5[a]	933.1[a]	933.3[a]	933.1[b]	933.1[c]
Cu $L\alpha$[d]	929.7	929.7	929.7	929.7	929.7
Cu 3d	3.8	3.4	3.6	3.4	3.4
VB (XPS)	3.7[e]	3.3[e]	3.5[a]	3.8[e]	3.5[c]
O 1s	529.5[a]	528.6[a]	528.5[a]	528.7[b]	528.7[c]
O $K\alpha$[d]	524.5	525.7	525.7	526.3	526.1
O 2p	5.0	2.9	2.8	2.4	2.6
VB (UPS)	4.6[e]	2.5[e]	2.8[f]	2.0[h]	3.2[g]

[a] Reference 1.
[b] Reference 2.
[c] Reference 52.
[d] This work.
[e] Reference 43.
[f] Reference 3.
[g] Reference 9.
[h] Reference 10.

ence emission lines (for further details see Ref. 21). The XPS core-level binding energies used to set the x-ray emission bands on a binding energy scale were taken from the literature and are summarized in Table I.

III. RESULTS

A. Cu *Lα*

In Fig. 2 we present the raw data for Cu *Lα* emission bands for La-Cu-O and the superconducting compounds on an x-ray transition energy scale. The Cu *Lα* spectrum from each compound is strikingly similar. In particular the Cu *Lα* peak positions are identically 929.7 eV. It is instructive to compare the width and shape of the same data for elemental copper and CuO (Fig. 3). The emission from the element has weak structure at 928 and 929 eV which compares well with peaks in the one-electron ground-state DOS (Ref. 29) at 3 and 4 eV binding energy [Fig. 3(c)]. Structure at higher x-ray transition energies in the elemental Cu spectrum is attributed to multiple ionization satellites, however.[30,31] They are irrelevant to the valence band DOS. Similar features centered at about 931 and 934 eV are also observed for the compounds. They explain the asymmetry of the Cu *Lα* emission bands. The amplitude of the 931 eV structure appears to increase as we go from La-Cu-O to Bi-Sr-Ca-Cu-O. We note, however, that it coincides in energy with the strong Cu L_3 absorption peak,[17] so its intensity will be very sensitive to self-absorption effects which, in turn, will depend critically on the composition of the material under study. This makes it difficult to establish whether there is a band-structure effect or not. In view of this, bandwidths are best estimated by fitting an appropriate function to the low-energy side of the spectrum. It turns out that a satisfactory fit is obtained using a Lorentzian profile with 2.0 eV full width at half maximum (FWHM) for all the high-T_c compounds but it is appreciably narrower (1.6 eV FWHM) for CuO.[21]

The difference in width between CuO and the high-T_c compounds, despite the same dominant structural feature of Cu atoms surrounded by four oxygens, may be related to the fact that the Cu-O units in CuO share a common edge (90° cation-anion-cation interaction) whereas they share a common corner in the other compounds (180° cation-anion-cation interaction). Figure 4 summarizes the theoretical Cu *d* DOS calculated from the full-potential linearized augmented-plane-wave (FLAPW) band structure.[32,33] Their shape changes appreciably as a

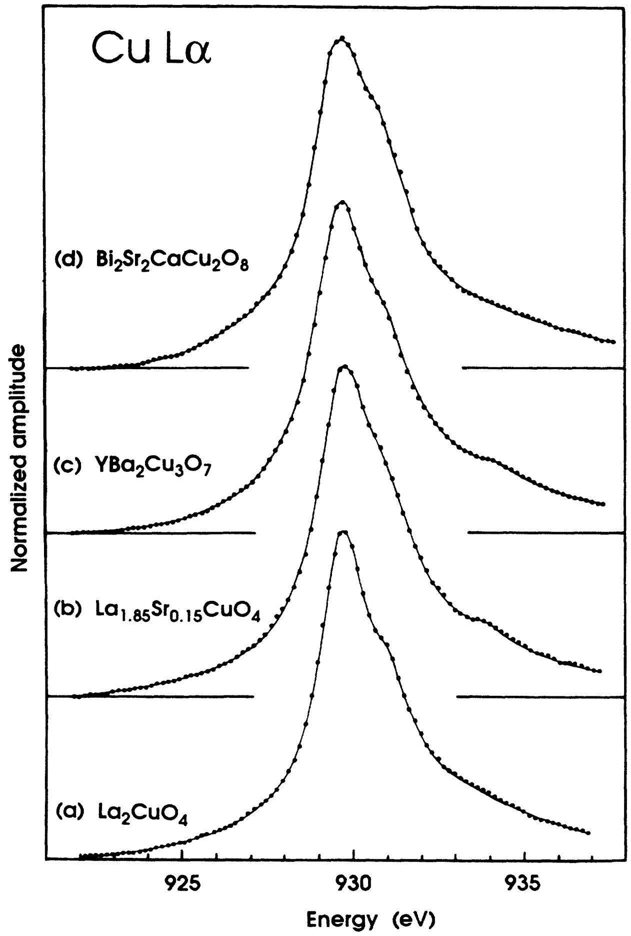

FIG. 2. Cu *Lα* emission band for La_2CuO_4 and three superconducting cuprates.

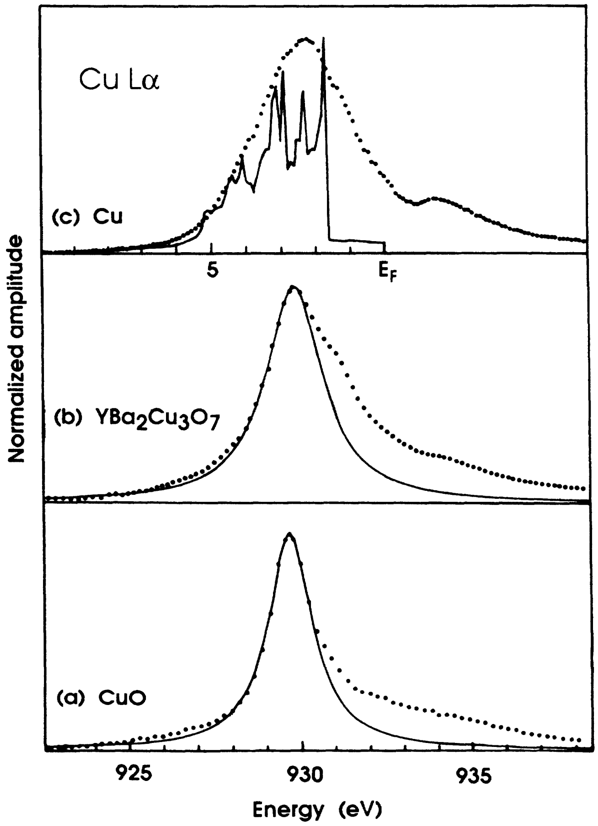

FIG. 3. Cu *Lα* emission band: (a) CuO; (b) $YBa_2Cu_3O_7$; (c) elemental copper. Also shown in (c) is the theoretical DOS taken from Ref. 29. Lorentzian fits are shown as a solid line.

function of the compound and has nothing in common with our observations.

B. O *K*α

In Fig. 5 we present the O *K*α emission band data. Here we note appreciable differences in shape and peak positions between compounds. Y-Ba-Cu-O and Bi-Sr-Ca-Cu-O give strongly asymmetric O *K*α bands with a relatively sharp cutoff towards higher x-ray energies, while La-Cu-O and La-Sr-Cu-O have almost symmetrical band shapes. The FWHM of the La-based compounds and Bi-Sr-Ca-Cu-O is ~3 eV; it is 2.6 eV for Y-Ba-Cu-O. In considering these values the restrictions concerning band shapes towards low energies mentioned in Sec. II must be borne in mind (so must the effect of self-absorption on the high-energy edge of these spectra). However, they remain significant taken comparatively. The emission bands peak at 525.7 eV for the two La compounds, and 526.3 and 526.1 eV for Y-Ba-Cu-O and Bi-Sr-Ca-Cu-O, respectively.

The significant differences in band shapes may be understood in terms of band-structure effects. In Fig. 6 we show the component O *p* DOS according to the FLAPW calculations.[32,33] For Cu-O plane oxygen states there is a dip between the *dp*σ bonding and antibonding states. In La-Cu-O this gap is filled in by the contribution from O(2) apical-oxygen states (this is also the case for the doped La compound[34]). In Y-Ba-Cu-O most of the weight is towards the Fermi energy (E_F) for all the oxygen sites. Bi-Sr-Ca-Cu-O differs from Y-Ba-Cu-O in two important respects: The O(3) apex oxygen lies closer to Cu than in Y-Ba-Cu-O (~2.05 Å instead of ~2.3 Å) and the oxygen in the Bi planes [O(2)] contribute a narrower band between the *dp*σ bonding and antibonding bands. In other words, the calculated DOS for oxygen sites which *do not* lie in the Cu-O planes can apparently

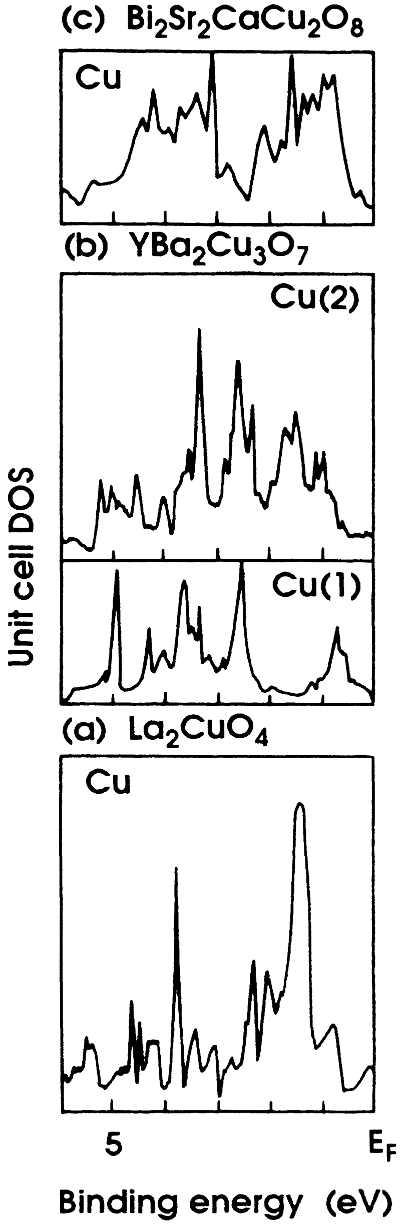

FIG. 4. Calculated local Cu *d* DOS per unit cell: La-Cu-O from Ref. 32; (b) Y-Ba-Cu-O [Cu(1): Cu-O chains; Cu(2): Cu-O planes] from Ref. 32; (c) Bi-Sr-Ca-Cu-O from Ref. 33.

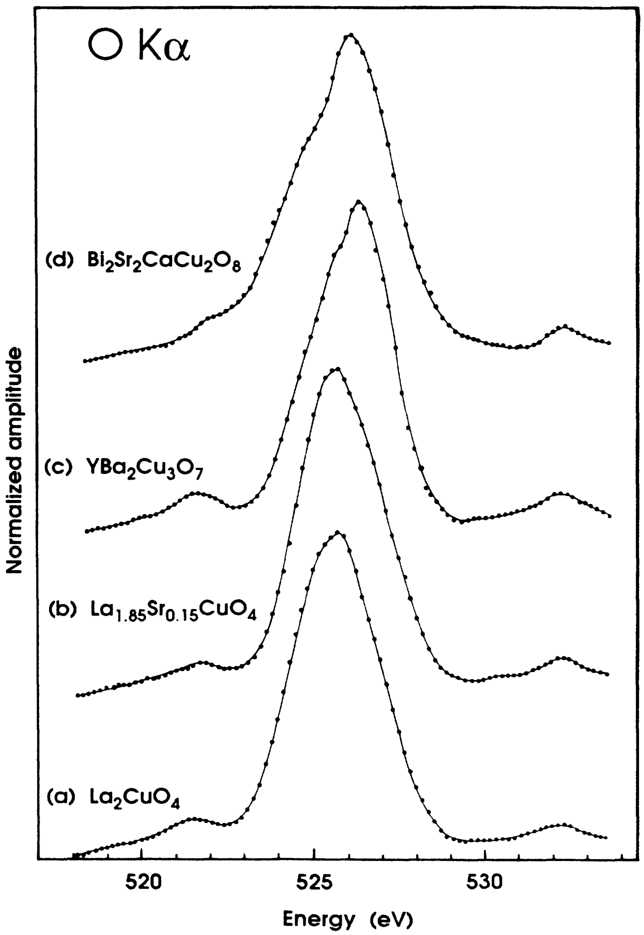

FIG. 5. O *K*α emission band for La_2CuO_4 and three superconducting cuprates.

explain the differences observed in the O $K\alpha$ bands for the three types of compound.

IV. DISCUSSION

So far we have shown that the main features of the spectra can be qualitatively explained in terms of the gross structural differences, but that there are major discrepancies between LDA calculations and these experiments especially as far as the Cu-site d states are concerned. In contrast to the broad Cu $3d$–O $2p$ hybridization of the LDA ground state, the Cu $L\alpha$ spectra show rather well localized Cu $3d$ states. Independently from arguments concerning the validity of the LDA description, there are two possible reasons for this major discrepancy. One may be that the ground state cannot serve as a good approximation to the excitation spectrum because on-site Coulomb interaction is large (see, for instance, Ref. 35). The other may be that the Cu $2p$ core hole initial state in the x-ray emission process may be an important perturbation.[36]

The effect of the initial core hole state in the x-ray emission process has been widely discussed in the literature (see, for instance, Ref. 37). The recurring assumption has been that even in d-electron compounds the final-state rule is applicable, i.e., in the case of x-ray emission the transition matrix element involves wave functions for the potential without the core hole. The approximation has been justified for transitions involving a free-electron-like band.[37] In other cases the justification rather lies with the difficulty of correctly dealing with the many-body problem. Very recently the XES Cu $3d \rightarrow 2p$ transition has been calculated by means of a Hamiltonian which includes the $2p$ core hole potential within the framework of the Anderson-impurity model.[36] It is calculated on the same footing as the Cu $2p$ x-ray absorption spectrum (XAS) and the Cu $2p$ and Cu $3d$ XPS spectra. In accord with XPS experiments, the theoretical Cu $2p$ core-level spectrum consists of two intense features. The more intense and least bound peak has the $2p^5 3d^{10}\,\underline{L}$ configuration ($\underline{L}$ indicates charge transfer from the ligand to the Cu site). The other corresponds to the $2p^5 3d^9$ configuration.[36] Both configurations contribute to the initial state of the x-ray emission which may thus reflect the sum of $3d^8$ and $3d^9\underline{L}$ final states. The two initial states are so well separated that they do not hybridize and both initial-to-final state energy differences are about equal so the two component emissions overlap.

If we can assume that the final state of the Cu $L\alpha$ emission consists mainly of $3d^9\underline{L}$ states,[20,36] it should give comparable information to photoelectron spectra. The O $K\alpha$ bands which as we have seen (Sec. II) relate well to the LDA O $2p$ partial DOS should also be comparable to the photoelectron spectra.

In fact as we have previously pointed out,[15,21] experimentally the $2p^5 3d^{10}\underline{L}$ XPS line is broader than the Cu $L\alpha$ signal in these compounds. Several explanations for its width have been given: juxtaposition of Cu^{+}, Cu^{2+}, and Cu^{3+} contributions,[38,39] delocalization of the ligand p band,[40] multiplet splitting,[41] or shake-up ($2p^5 3d^{10}\underline{L}^2$) and shake-down ($2p^5 3d^{10}$) satellites.[42] The fact that XES data are narrower than the XPS Cu $2p_{3/2}$ signal rather

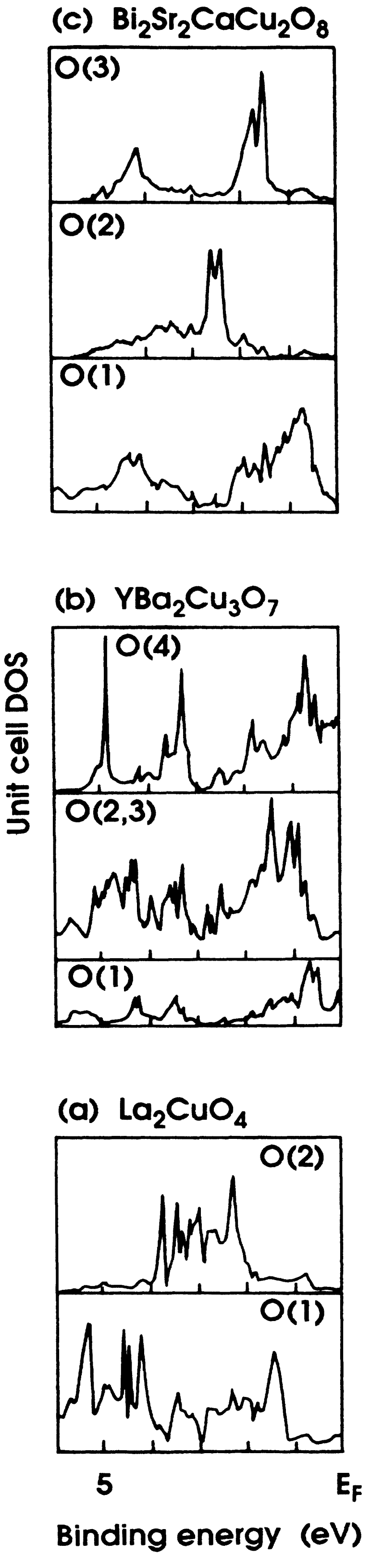

FIG. 6. Calculated local O p DOS per unit cell: (a) La-Cu-O [O(1): Cu-O planes; O(2): apical (La planes)] from Ref. 32; Y-Ba-Cu-O [O(1): Cu-O chains; O(2,3): Cu-O planes; O(4): apical] from Ref. 32; (c) Bi-Sr-Ca-Cu-O [O(1): Cu-O planes; O(2): Bi planes; O(3): apical (Sr planes)] from Ref. 33.

accredits one of the latter two explanations.

To compare our spectra with PES data we have placed the Cu $L\alpha$ and O $K\alpha$ emission bands on a binding energy scale using the XPS Cu $2p_{3/2}$ (main line) and O $1s$ core-level binding energies (Table I). For the high-T_c compounds the Cu $L\alpha$ emission bands lie at ~3.4 eV and this value agrees well with the XPS valence band spectra which are dominated by states with d symmetry.[43] In Figs. 7 and 8 we compare our data with high quality PES measurements taken at 50 eV photon energy on single crystals of, respectively, Y-Ba-Cu-O (Ref. 10) and Bi-Sr-Ca-Cu-O (Ref. 9) cleaved and maintained at very low temperatures and with the FLAPW and total DOS for Y-Ba-Cu-O (Ref. 44) and Bi-Sr-Ca-Cu-O (Ref. 33).

The main valence band intensity for Y-Ba-Cu-O, with background subtracted, is situated at 2.0 eV.[10] This agrees quite well with the O $K\alpha$ peak position at 2.4 eV. For Bi-Sr-Ca-Cu-O the main O $2p$ intensity according to our x-ray data is at 2.6 eV with a shoulder at 3.5 eV. The main peak in the photoelectron spectrum this time lies at about 3.2 eV,[9] i.e., above the XES value. Constant-initial-state (CIS) photoelectron spectroscopy performed to help identify the character of the spectral features of the Bi-Sr-Ca-Cu-O valence band shows resonances at initial state energies (E_i) of 1.5 and 2.8 eV for photon energies in the region of the O $2s$ ionization threshold.[45] This clearly identifies the energy position of the main O $2p$ components. On the other hand CIS data taken at $E_i = 3.2$ eV show a slight dip in intensity at the Cu $3p$ threshold indicating a relatively low $3d$ DOS in this region.[46] FLAPW DOS calculations (Fig. 6) indicate that the O(1) (Cu-O plane), O(2) (Bi-O plane), and O(3) (Cu-O apex) $2p$ states peak at ~1, ~2.6, and ~1.7 eV, respectively. If the FLAPW DOS are shifted 0.5–1 eV to obtain a better fit with experiments, we can conclude that the O $2p$ states which contribute to the intensity at 3.2 eV in the low-energy PES data are mainly from O(2) states. The fact that these O(2) states only appear as a shoulder in the O $K\alpha$ band and that the Cu $L\alpha$ emission situates the $3d$ states at 3.4 eV suggests that both Cu $3d$ and O(2) $2p$ states contribute to the photoelectron spectrum at 3.2 eV.

Thus from the above arguments we can tentatively assume that, subject to appropriate allowance for cross section effects, the Cu $3d$ and O $2p$ final states probed separately by XES are indeed those probed by PES and that the perturbation caused by the core hole in the initial state of the x-ray emission process is small. As opposed to earlier data, the very recent photoelectron spectra shown in Figs. 7 and 8 provide much improved agreement between one-electron ground-state band-structure calculations and experiment.[9,10] This kind of agreement is in fact what we[15] and others[22] have established for the O $K\alpha$ emission band data and O $2p$ partial DOS.

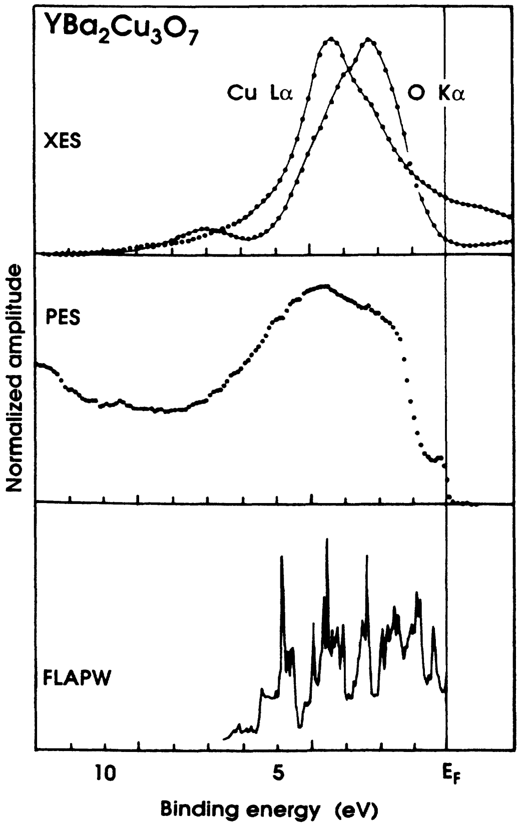

FIG. 7. Cu $L\alpha$ and O $K\alpha$ emission bands (top panel), PES valence band taken from Ref. 10 (middle panel), and DOS taken from Ref. 44 for $YBa_2Cu_3O_7$ (bottom panel).

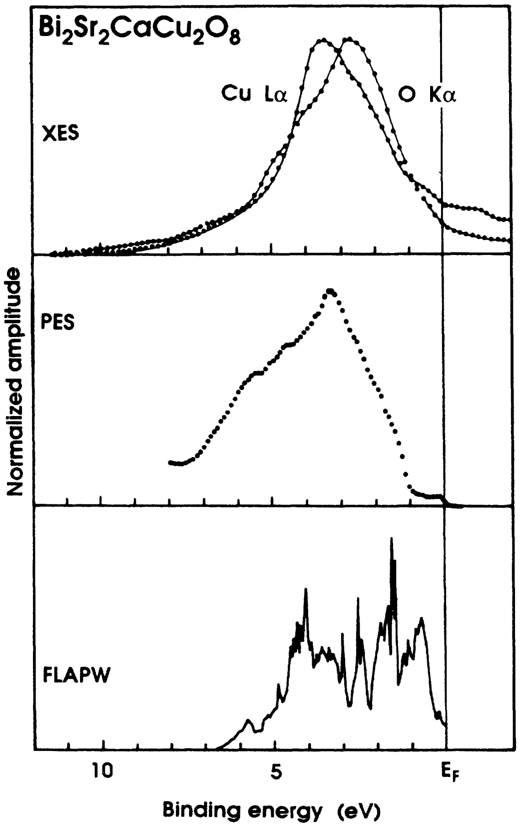

FIG. 8. Cu $L\alpha$ and O $K\alpha$ emission bands (top panel), PES valence band taken from Ref. 9 (middle panel), and DOS taken from Ref. 33 for $Bi_2Sr_2CaCu_2O_8$ (bottom panel).

Thus it appears that the two main obstacles to considering that the excitation spectra of these cuprates are adequately described by LDA (at least in their metallic phases) are the photoelectron spectrum satellite at ~12 eV which is known to have d character and the Cu $L\alpha$ spectrum which appears to reflect a narrow $3d$ band. Unfortunately, attempts to include on-site d-d Coulomb interaction to account for the extra hole in the excitation spectrum within the framework of LDA are in a too early stage of development to justify confrontation with our results. Hence we look more closely at alternative approaches already capable of treating a two-hole system in the presence of large Coulomb interaction, namely the Anderson-impurity model[3,36,47,48] and cluster method.[49,50]

In this respect CuO serves as a convenient prototype for the superconductors insofar as they can be described by a $(CuO_4)^{6-}$ cluster in D_{4h} symmetry. In Fig. 9 we give the Cu $L\alpha$ emission band of CuO (Ref. 21) compared to the FLAPW $3d$ DOS,[32] the XPS spectrum,[43] the d spectral weight of a cluster calculation,[50] and an Anderson-impurity model.[47] As mentioned in Sec. III we would expect a strong localization of the Cu $3d$ states even in the bulk materials from the 90° Cu-O-Cu bonding which for instance means that the $d_{x^2-y^2}$ orbitals from neighboring Cu atoms hybridize with different (orthogonal) O $p_{x,y}$ orbitals. It follows that the absence of translational symmetry inherent in the cluster model is not as drastic an approximation for CuO as in the high-T_c compounds where the $3d$ band is expected to be more dispersive as a result of 180° bonding.

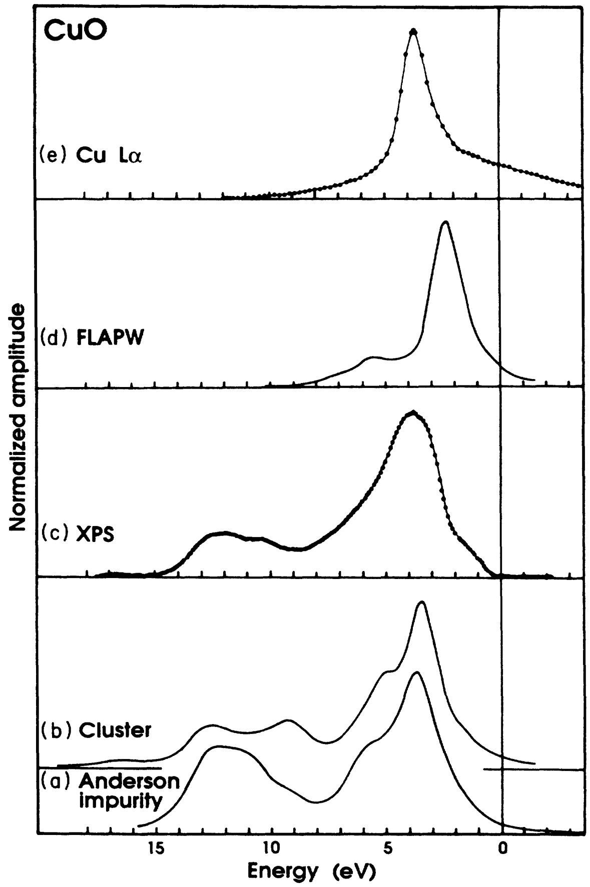

FIG. 9. CuO calculated $3d$ XPS valence band: (a) Anderson-impurity model (Ref. 36); (b) cluster model (Ref. 50). Also shown are (c) the experimental Mg $K\alpha$-induced XPS spectrum (Ref. 43); (d) the FLAPW d DOS (Ref. 32); (e) the Cu $L\alpha$ emission band (this work).

Indeed the FLAPW d DOS for CuO (Ref. 32) correctly predict the strong localization of the Cu $3d$ states but the main peak lies too close to E_F compared with both XPS and XES data. Furthermore a high-binding-energy shoulder is predicted but not observed in the Cu $L\alpha$ spectrum.

The obvious advantage of both the cluster calculation and the Anderson-impurity calculation is that they correctly predict, at least qualitatively, the $3d^8$ final state satellite, but little can be asserted concerning energy positions because of the large number of adjustable parameters required. Eskes *et al.*[50] show that if the Coulomb interaction is set to zero, the d-spectral weight from the cluster calculation is in excellent agreement with an LDA DOS calculation.[50,51] They both show up the high-binding-energy shoulder in the d states [Figs. 9(a) and 9(b)] which coincides with the main peak in the O p states. In the two-hole XPS excitation spectrum calculated with the cluster model there is a weak shoulder to the low-binding-energy side of the main peak and a broader, more intense shoulder to the high-binding-energy side. Similar features are found in the Anderson-impurity calculation.[47] An analysis of the eigenstates performed by Eskes *et al.*[50] shows that the main peak and shoulder correspond to $3d^9\underline{L}$ final states. Thus we would expect a shoulder to show up in the Cu $L\alpha$ spectrum, whereas in fact only a very weak hump is observed ~3 eV below its peak position [see Fig. 3(a)].

Using the arguments put forward by Tanaka *et al.* to describe the Cu $L\alpha$ emission from La-Cu-O,[36] and assuming the D_{4h} symmetry, we note that the initial states of the x-ray emission process must be $2p^5 3d^9(b_{1g})$ and $2p^5 3d^{10}\underline{L}(b_{1g})$. The notation indicates that the hole has b_{1g} symmetry and that it is either on a Cu $3d_{x^2-y^2}$ orbital (in which case the initial state is subject to the strong on-site Coulomb interaction between the core hole and the valence hole) or is on a ligand site. The largest contribution to the valence DOS comes from the d_ϵ states (d_ϵ stands for degenerate b_{2g} and e_g symmetry states related to the $3d_{xy}$ and $3d_{xz,yz}$ orbitals).

In the Cu-site x-ray emission process the $2p^5 3d^{10}\underline{L}(b_{1g})$ initial state will mainly give rise to a $3d^9(d_\epsilon)\underline{L}(b_{1g})$ final state while $3d^9(b_{1g})\underline{L}(d_\epsilon)$ will have negligible probability. Thus the Cu $L\alpha$ emission picks out primarily the d_ϵ states and this explains why a single peak is observed. The XPS spectrum on the other hand includes contributions from both $3d^9(b_{1g})\underline{L}(d_\epsilon)$ and $3d^9(d_\epsilon)\underline{L}(b_{1g})$ configurations which will give rise to two peaks if $\Delta d_\epsilon \neq \Delta b_{1g}$ [$\Delta d_\epsilon(\Delta b_{1g})$ is the charge-transfer energy which concerns the transfer of $d_\epsilon(b_{1g})$ from the ligand to the Cu site].

The parameters which go into the calculation of the XES spectrum for La-Cu-O (Ref. 36) were chosen to give the best description of the 3d XPS and Cu 2p XAS data.[47] According to Ref. 47, Δd_ϵ is 4.5 eV for CuO as opposed to 3.0 eV for La-Cu-O. This means that hybridization with the $3d^{10}\underline{L}^2(d_\epsilon, b_{1g})$ configuration is smaller in CuO than La-Cu-O. It could be that the hump observed in the CuO spectrum ~3 eV below the main peak results from weak hybridization between $3d^9\underline{L}$ and $3d^{10}\underline{L}^2$ configurations. The fact that such structure is not apparent in the other cuprates might then be due to the smaller values of Δd_ϵ and the concomitant increase in bandwidth.

A tight-binding (TB) parametrization of the band structure (see Ref. 52) can be helpful in understanding some of the complex electronic properties of the high-T_c compounds. De Weert *et al.*,[53] from a TB fit to an LAPW calculation, have obtained the fully decomposed Cu $d_{x^2-y^2}$, $d_{3z^2-r^2}$, and $d_{xy,xz,yz}$ DOS for La-Cu-O along with the O 2p DOS. They are perfectly compatible with the molecular orbital theory model discussed above: The unoccupied states have essentially $d_{x^2-y^2}$ character, the $d_{3z^2-r^2}$ orbitals form a sharp peak just below E_F and the $d_{xy,xz,yz}$ states lie in a 1.3-eV-wide band mainly ~2.0 eV below E_F. The latter is only very weakly hybridized with the O p states.

In summary therefore our XES data indicate that the O 2p states can be regarded as bandlike and as such are well described by LDA theory. On the other hand a coherent understanding of the Cu ($3d \rightarrow 2p$) x-ray emission process is possible only if on-site $d-d$ Coulomb interaction is taken into account. Our data are compatible with the findings of Tanaka *et al.*[36] who, using an Anderson-impurity model, suggest that the Cu $L\alpha$ emission band provides information on the $d_{xy,xz,yz}$ states in a two-hole excitation spectrum. As such these experiments should help in establishing the validity of band-structure-based models at present being developed to include on-site Coulomb interaction.

ACKNOWLEDGMENTS

Laboratoire de Chimie Physique and Laboratoire de Cristallographie et Sciences des Matériaux are Unités Associées au Centre National de la Recherche Scientifique (CNRS).

---

[1] N. Nücker, J. Fink, B. Renker, D. Ewert, C. Politis, P. J. W. Weijs, and J. C. Fuggle, Z. Phys. B **67**, 9 (1987).

[2] P. Steiner, V. Kinsinger, I. Sander, B. Siegwart, S. Hüfner, and C. Politis, Z. Phys. B **67**, 19 (1987).

[3] Z.-X. Shen, J. W. Allen, J. J. Yeh, J. S. Kang, W. Ellis, W. Spicer, I. Lindau, M. B. Maple, Y. D. Dalichaouch, M. S. Toukachvili, J. Z. Sun, and T. H. Geballe, Phys. Rev. B **36**, 8414 (1987).

[4] J. C. Fuggle, P. J. W. Weijs, R. School, G. A. Sawatzky, J. Fink, N. Nücker, P. J. Durham, and W. M. Temmerman, Phys. Rev. B **37**, 123 (1988).

[5] J. H. Weaver, H. M. Meyer III, T. J. Wagener, D. M. Hill, Y. Gao, D. Peterson, Z. Fisk, and A. J. Arko, Phys. Rev. B **38**, 4668 (1988).

[6] J.-M. Imer, F. Patthey, B. Dardel, W.-D. Schneider, Y. Baer, Y. Petroff, and A. Zettl, Phys. Rev. Lett. **62**, 336 (1989).

[7] Y. Chang, Ming Tang, R. Zanoni, M. Onellion, R. Joynt, D. L. Huber, G. Margaritondo, P. A. Morris, W. A. Bonner, J. M. Tarascon, and N. G. Stoffel, Phys. Rev. B **39**, 4740 (1989).

[8] R. Manzke, T. Buslaps, R. Claessen, and J. Fink, Europhys. Lett. **9**, 477 (1989).

[9] R. S. List, A. J. Arko, R. J. Bartlett, C. G. Olson, A.-B. Yang, R. Liu, C. Gu, B. W. Veal, Y. Chang, P. Z. Jiang, K. Vandervoort, A. P. Paulikas, and J. C. Campuzano, Physica **159C**, 439 (1989).

[10] A. J. Arko, R. S. List, R. J. Bartlett, S.-W. Cheong, Z. Fisk, J. D. Thompson, C. G. Olson, A.-B. Yang, R. Liu, C. Gu, B. W. Veal, J. Z. Liu, A. P. Paulikas, K. Vandervoot, H. Claus, J. C. Campuzano, J. E. Schirber, and N. D. Shinn, Phys. Rev. B **40**, 2268 (1989).

[11] M. S. Hybersten, M. Schlüter, and N. E. Christensen, Phys. Rev. B **39**, 9028 (1989).

[12] A. K. McMahan, R. M. Martin, and S. Satpathy, Phys. Rev. B **38**, 6650 (1989).

[13] L. F. Mattheiss and D. R. Hamann, Phys. Rev. B **40**, 2217 (1989).

[14] T. M. Rice, Z. Phys. B **67**, 141 (1987).

[15] C. F. Hague, V. Barnole, J.-M. Mariot, C. Michel, and B. Raveau, in *High-T_c Superconductors: Electronic Structure*, edited by A. Bianconi and A. Marcelli (Pergamon, Oxford, 1989), p. 325.

[16] J.-M. Mariot, V. Barnole, C. F. Hague, V. Geiser, and H.-J. Güntherodt, Solid State Commun. **64**, 1203 (1987).

[17] J.-M. Mariot, V. Barnole, C. F. Hague, V. Geiser, and H.-J. Güntherodt, J. Phys. (Paris) **48**, C9-1203 (1987).

[18] K.-L. Tsang, C. H. Zhang, T. A. Callcott, L. R. Canfield, D. L. Ederer, J. E. Blendell, C. W. Clark, N. E. Wassdahl, J. E. Rubensson, G. Bray, N. Mårtensson, J. Nordgren, R. Nyholm, and S. Cramm, J. Phys. (Paris) **48**, C9-1193 (1987).

[19] V. I. Anisinov, V. R. Galakhov, E. Z. Kurmaev, M. A. Korotin, V. L. Kozhevnikov, and G. V. Bazuev, Fiz. Met. Metalloved. **65**, 207 (1988).

[20] V. Barnole, J.-M. Mariot, C. F. Hague, and H.-J. Güntherodt, Physica **153-155C**, 125 (1988).

[21] J.-M. Mariot, V. Barnole, C. F. Hague, G. Vetter, and F. Queyroux, Z. Phys. B **75**, 1 (1989).

[22] C. H. Zhang, T. A. Callcott, K.-L. Tsang, D. L. Ederer, J. E. Blendell, C. W. Clark, T. Scimeca, and Y.-W. Liu, Phys. Rev. B **39**, 4796 (1989).

[23] C. Michel, J. Deslandes, J. Provost, P. Lejay, R. Tournier, M. Hervieu, and B. Raveau, C. R. Acad. Sci. Paris **304-II**, 1059 (1987).

[24] J. Beille, R. Cabanel, C. Chaillout, B. Chevalier, G. Demazeau, F. Deslandes, J. Etourneau, P. Lejay, C. Michel, J. Provost, B. Raveau, A. Sulpice, J.-L. Tholence, and R. Tournier, C. R. Acad. Sci. Paris **304-II**, 1097 (1987).

[25] C. F. Hague and D. Laporte, Rev. Sci. Instrum. **51**, 621 (1980).

[26] J. Valjakka, J. Utriainen, T. Åberg, and J. Tulkki, Phys. Rev. B **32**, 6892 (1985).

[27] D. W. Fischer, J. Chem. Phys. **42**, 3814 (1965).

[28] D. M. Barrus, R. L. Blake, A. J. Burek, K. C. Chambers, and L. E. Cox, Phys. Rev. B **22**, 4022 (1980).

[29] V. L. Moruzzi, J. F. Janak, and A. R. Williams, *Calculated Electronic Properties of Metals* (Pergamon, New York, 1978).

[30] C. F. Hague, J.-M. Mariot, and H. Ostrowiecki, Jpn. J. Appl. Phys. **17** (2), 105 (1978).

[31] J. Nordgren, J. Phys. (Paris) **48**, C9-693 (1987).

[32] K. T. Park, K. Terakura, T. Oguchi, A. Yanase, and N. Ikeda, J. Phys. Soc. Jpn. **57**, 3445 (1989).

[33] S. Massidda, Jaejun Yu, and A. J. Freeman, Physica **152C**, 251 (1988).

[34] G. M. Stocks, W. M. Temmerman, Z. Szotek, P. A. Sterne, and P. L. Fejes, Supercond. Sci. Technol. **1**, 57 (1988).

[35] M. R. Norman and A. J. Freeman, Phys. Rev. B **33**, 8896 (1986).

[36] S. Tanaka, K. Okada, and A. Kotani, J. Phys. Soc. Jpn. **58**, 813 (1989).

[37] U. von Barth and G. Grossmann, Phys. Rev. B **25**, 5150 (1982).

[38] P. Steiner, S. Hüfner, V. Kinsinger, I. Sander, B. Siegwart, H. Schmitt, R. Schulz, S. Junk, G. Schwitzgebel, A. Gold, C. Politis, H. P. Müller, R. Hoppe, S. Kemmler-Sack, and C. Kunz, Z. Phys. B **69**, 449 (1988).

[39] P. Sen, B. Dauth, T. Kachel, B. Rupp, and W. Gudat, Physica **153-155C**, 153 (1988).

[40] F. U. Hillebrecht, J. Fraxedas, L. Ley, H. J. Trodahl, J. Zaanen, W. Braun, M. Mast, H. Petersen, M. Schaible, L. C. Bourne, P. Pinsukanjana, and A. Zettl, Phys. Rev. B **39**, 236 (1989).

[41] K. Okada and A. Kotani, J. Phys. Soc. Jpn. **58**, 2578 (1989).

[42] G. Wendin, Phys. Scr. T **27**, 31 (1989).

[43] P. Steiner, S. Hüfner, A. Jungmann, V. Kinsinger, and I. Sander, Z. Phys. B **74**, 173 (1989).

[44] S. Massidda, Jaejun Yu, A. J. Freeman, and D. D. Koelling, Phys. Lett. A **122**, 198 (1987).

[45] R. Manzke, T. Buslaps, R. Claessen, G. Mante, and Z. X. Zhao, Solid State Commun. **70**, 67 (1989).

[46] Z.-X. Shen, P. A. P. Lindberg, P. Soukassian, C. B. Eom, I. Lindau, W. E. Spicer, and T. H. Geballe, Phys. Rev. B **39**, 823 (1989).

[47] K. Okada and A. Kotani, J. Phys. Soc. Jpn. **58**, 1095 (1989).

[48] J. Zaanen and G. A. Sawatzky, Can. J. Phys. **65**, 1262 (1987).

[49] A. Fujimori, E. Takayama-Muromachi, and Y. Uchida, Solid State Commun. **63**, 857 (1987).

[50] H. Eskes, L. H. Tjeng, and G. A. Sawatzky (unpublished).

[51] J. Ghijsen, L. H. Tjeng, J. van Elp, H. Eskes, J. Westerink, G. A. Sawatzky, and M. T. Czyzyk, Phys. Rev. B **38**, 11 322 (1988).

[52] W. E. Pickett, Rev. Mod. Phys. **61**, 433 (1989).

[53] M. J. De Weert, D. A. Papaconstantopoulos, and W. E. Pickett, Phys. Rev. B **39**, 4235 (1989).